

AD-A131 825

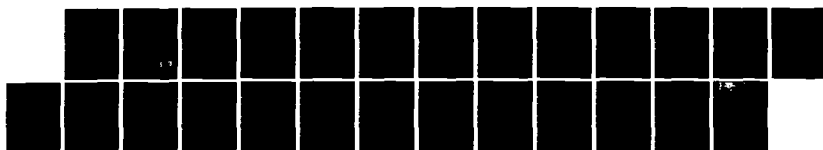
THE OWENS VALLEY FREQUENCY-AGILE INTERFEROMETER(U)
CALIFORNIA INST OF TECH PASADENA G J HURFORD MAR 83
SCIENTIFIC-1 AFGL-TR-83-0108 F19628-82-K-0033

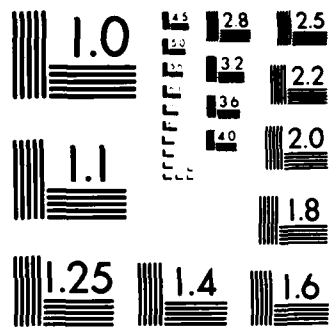
1/1

UNCLASSIFIED

F/G 20/6

NL





MICROCOPY RESOLUTION TEST CHART
NATIONAL BUREAU OF STANDARDS-1963-A

12

AFGL-TR-83-0108

THE OWENS VALLEY FREQUENCY-AGILE
INTERFEROMETER

G.J. Hurford

California Institute of Technology
1201 E. California Blvd.
Pasadena, CA 91125

Scientific Report No. 1

March 1983

Approved for public release; distribution unlimited

AIR FORCE GEOPHYSICS LABORATORY
AIR FORCE SYSTEMS COMMAND
UNITED STATES AIR FORCE
HANSCOM AFB, MASSACHUSETTS 01731

DTIC
ELECT
AUG 25 1983
S A

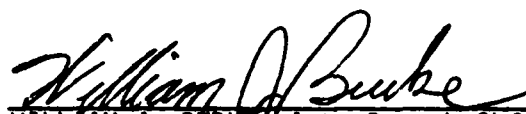
DTIC FILE COPY

83 08 23 101


This report has been reviewed by the ESD Public Affairs Office (PA) and is releasable to the National Technical Information Services (NTIS).

"This technical report has been reviewed and is approved for publication"


EDWARD W. CLIVER
Contract Manager


WILLIAM J. BURKE, Actg Branch Chf
Plasmas, Particles & Fields Branch
Space Physics Division

FOR THE COMMANDER


RITA C. SAGALYN, Director
Space Physics Division

Qualified requestors may obtain additional copies from the Defense Technical Information Center. All others should apply to the National Technical Information Service.

If your address has changed, or if you wish to be removed from the mailing list, or if the addressee is no longer employed by your organization, please notify AFGL/DAA, Hanscom AFB, MA 01731. This will assist us in maintaining a current mailing list.

Do not return copies of this report unless contractual obligations or notices on a specific document requires that it be returned.

Unclassified

SECURITY CLASSIFICATION OF THIS PAGE (When Data Entered)

REPORT DOCUMENTATION PAGE		READ INSTRUCTIONS BEFORE COMPLETING FORM
1. REPORT NUMBER AFGL-TR-83-0108	2. GOVT ACCESSION NO. AD-A131 825	3. REPORT NUMBER RECIPIENT'S CATALOG NUMBER
4. TITLE (and Subtitle) THE OWENS VALLEY FREQUENCY-AGILE INTERFEROMETER		5. TYPE OF REPORT & PERIOD COVERED Scientific Report No. 1
		6. PERFORMING ORG. REPORT NUMBER
7. AUTHOR(s) G. J. Hurford		8. CONTRACT OR GRANT NUMBER(s) F19628-82-K-0033
9. PERFORMING ORGANIZATION NAME AND ADDRESS California Institute of Technology 1201 E. California Blvd. Pasadena, CA 91125		10. PROGRAM ELEMENT, PROJECT, TASK AREA & WORK UNIT NUMBERS 2311G3FH 611021F
11. CONTROLLING OFFICE NAME AND ADDRESS Air Force Geophysics Laboratory Hanscom AFB, Massachusetts 01731 Monitor/Edward Cliver PHG		12. REPORT DATE March 1983
		13. NUMBER OF PAGES 22
14. MONITORING AGENCY NAME & ADDRESS (if different from Controlling Office)		15. SECURITY CLASS. (of this report) Unclassified
		15a. DECLASSIFICATION/DOWNGRADING SCHEDULE
16. DISTRIBUTION STATEMENT (of this Report) Approved for public release; distribution unlimited		
17. DISTRIBUTION STATEMENT (of the abstract entered in Block 20, if different from Report)		
18. SUPPLEMENTARY NOTES		
19. KEY WORDS (Continue on reverse side if necessary and identify by block number) Sun Flares Solar radio emission Frequency-Agile interferometry		
20. ABSTRACT (Continue on reverse side if necessary and identify by block number) The Solar microwave spectrum encodes significant information on plasma parameters, magnetic field strengths and characteristics of accelerated electrons in solar flares and active regions. To fully exploit this source of diagnostic information requires microwave observations with considerably better spectral resolution than typically obtained to date. To accomplish this, the solar interferometer of the Owens Valley Radio Observatory has		

Unclassified

SECURITY CLASSIFICATION OF THIS PAGE (When Data Entered)

Unclassified

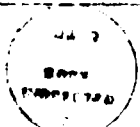
SECURITY CLASSIFICATION OF THIS PAGE (When Data Entered)

20. recently been converted to frequency-agile operation to effectively become a high resolution, interferometric spectrometer.

The interferometer uses two moveable, 27 m diameter parabolic antennas equipped with frequency-agile receivers. These receivers are capable of switching their observing frequency in less than 50 ms between any of 86 different frequencies in the range 1 to 18 GHz. The receivers have feeds which can be interchanged in less than 500 ms to permit observations in either right or left circular polarization. Observations consist of observer-defined frequency/polarization sequences in which successive integration periods of 50 or 100 ms can be used for observing or for frequency/polarization changes. Each measurement provides information equivalent to the amplitude and phase of the interferometric signal as well as the total power from each antenna. All data are absolutely calibrated with respect to cosmic sources.

In 1981, observations with one frequency-agile receiver were conducted and high resolution spectra of many flares were obtained. One unexpected aspect of such spectra were "narrow-band" bursts, which featured sharp high- and low-frequency cutoffs and a relatively narrow bandwidth. These events were found to occur both in isolation and as the early stages of much larger bursts with conventionally wide bandwidths. Examples of such events are shown and their implications discussed.

Accession No.	
BIOGRAPHICAL	
DIST. 1	
ELECTRONIC	
CLASSIFICATION	
BY	
DATE	
APPROVED	
Dist	



Unclassified

SECURITY CLASSIFICATION OF THIS PAGE (When Data Entered)

THE OWENS VALLEY FREQUENCY-AGILE INTERFEROMETER

G. J. Hurford

California Institute of Technology

ABSTRACT

The solar microwave spectrum encodes significant information on plasma parameters, magnetic field strengths and characteristics of accelerated electrons in solar flares and active regions. To fully exploit this source of diagnostic information requires microwave observations with considerably better spectral resolution than typically obtained to date. To accomplish this, the solar interferometer of the Owens Valley Radio Observatory has recently been converted to frequency-agile operation to effectively become a high resolution, interferometric spectrometer.

The interferometer uses two moveable, 27 m diameter parabolic antennas equipped with frequency-agile receivers. These receivers are capable of switching their observing frequency in less than 50 ms between any of 86 different frequencies in the range 1 to 18 GHz. The receivers have feeds which can be interchanged in less than 500 ms to permit observations in either right or left circular polarization. Observations consist of observer-defined frequency/polarization sequences in which successive integration periods of 50 or 100 ms can be used for observing or for frequency/polarization changes. Each measurement provides information equivalent to the amplitude and phase of the interferometric signal as well as the total power from each antenna. All data are absolutely calibrated with respect to cosmic sources.

In 1981, observations with one frequency-agile receiver were conducted and high resolution spectra of many flares were obtained. One unexpected aspect of such spectra were "narrow-band" bursts, which featured sharp high- and low-frequency cutoffs and a relatively narrow bandwidth. These events were found to occur both in isolation and as the early stages of much larger bursts with conventionally wide bandwidths. Examples of such events are shown and their implications discussed.

I. INTRODUCTION

The frequency dependence of solar microwave emission has been a relatively neglected aspect of solar spectroscopy. Most of the microwave spectral information we possess has been acquired by comparison of independent, single-frequency observations, often made with separate telescopes. Although carefully conducted, such measurements have been limited to typically one data point every octave (viz. frequency-resolution $df/f \sim 1$).

There are exceptions to this pattern. High spectral resolution measurements have been reported by Soviet workers using the RATAN-600 telescope between 5 and 7 GHz (Kaverin et al. 1979). At lower frequencies the dynamic spectra of decimetric bursts has been observed with high frequency and time resolution (Kruger 1979), but with intensities usually uncalibrated. In general at microwave frequencies, however, there has been an almost total absence of high spectral resolution solar data, and a complete absence of such data with polarization and spatial resolution.

This gap in our observational view of the sun is unfortunate for the microwave spectrum encodes important information, particularly for studies of solar activity. For example, the spectrum of gyrosynchrotron emission from the impulsive phase of flares reflects particle and plasma properties at the acceleration region. The high and low frequency slopes and turnover frequency of the total emission intensity as well as the polarization spectrum depend on the local magnetic field strength and direction, and on the spectral and spatial distribution of the emitting non-thermal particles (e.g. Dulk and Marsh 1982).

In the preflare active region, spatially resolved observations at single frequencies have established that one of the features of active region emission at microwave frequencies are compact, optically thick sources with coronal brightness temperatures (for reviews, see Schmahl, 1980; Marsh and Hurford, 1982). Such sources are due to gyroresonance opacity which provides large optical depths at frequencies which are low multiples of the local gyrofrequency. Since the gyrofrequency is determined solely by the magnetic field, the frequency dependence of microwave emission from solar active regions is very sensitive to the coronal magnetic field. For this to be observed and fully exploited as a probe of solar activity, sufficient spectral resolution is required to distinguish the gyroresonant harmonics, and spatial resolution is needed to isolate these small sources from the background sun.

Motivated by such considerations, the solar interferometer at the Owens Valley Radio Observatory (OVRO) has recently been converted to frequency-agile operation to permit high resolution interferometric microwave spectroscopy over the frequency range of 1 to 18 GHz. The purpose of this paper is to describe the hardware developed to accomplish such measurements, and to illustrate it with selected flare spectra. In section II, an overview of the interferometer concept is given with the frequency-agile receivers described in more detail in Section III. Data processing and calibration considerations are discussed in Section IV. Section V presents some microwave flare spectra obtained during 1981, summarizes the development of the interferometer, and outlines future plans.

II. OVERVIEW OF THE FREQUENCY-AGILE INTERFEROMETER

The Solar Interferometer is based on the 27 m antennas and associated systems of the OVRO centimetric interferometer. In 1976 new receivers and associated hardware were developed to meet the distinct requirements for solar observations (Zirin, Hurford and Marsh 1978). In 1979 the time resolution was upgraded from 1 s to 25, 50 or 100 ms (switch-selectable). In this form, the system provided high time resolution interferometric data at 10.6 GHz during the Solar Maximum Year.

The conversion of the system from a fixed-frequency interferometer to a microwave spectrometer is based on the concept of frequency-agility. This makes use of receivers that can be quickly tuned over a wide range so that successive measurements can be made at different frequencies. If this can be done sufficiently rapidly that the incident spectrum does not change appreciably, then detailed measurements of the solar microwave spectrum can be conveniently obtained with a single instrument.

The interferometer consists of three major subsystems: antennas, receivers, and the backend signal processing hardware. The operation of these subsystems are controlled and coordinated by a PDP-11/20 minicomputer. Figure 1 provides an overview of the system for the case of the 2-element interferometer.

The antennas are fully steerable, 27 m diameter paraboloids, originally built in 1958 and subsequently upgraded. Their equatorial mounts provide an hour angle range of ± 4 hours (less for declinations below -20 degrees). Pointing is controlled by the computer which issues appropriate velocity commands after comparing the

desired antenna position to the current position as indicated by encoder readouts. The antennas can be moved to any of 18 stations (Figure 2) to provide a wide range of baselines up to 600 m east-west or 500 m north-south. For three element interferometry, the OVRO 40 m antenna can be included. This combination can provide baselines of up to 1.25 km east-west which corresponds to a resolution (fringe spacing) of 2.75 arcseconds at 18 GHz.

The frequency-agile receivers are mounted at the prime focus of each antenna. Coarse tuning of the receivers is controlled by the computer while precise frequency control is maintained by 200 MHz and 1 MHz reference frequencies generated in the control building. The receiver outputs are delayed to compensate for different source to antenna geometries, and then returned to the control room where they are filtered, amplified, summed, and detected (Figure 1).

The 1 MHz reference signals that are sent to the receivers are deliberately offset by 500 Hz. Since they are linearly related to the observing frequency, the detected (antenna-summed) signal contain a 500 Hz component which is due to the coherent interference of the signals from the separate antennas. (This is in addition to a DC component which represents the total microwave power.) The correlated signal component is separately amplified with a switch-selectable "fringe gain" and then measured in phase quadrature. Each measurement yields the total power from each antenna, the COSINE (or REAL) component of the correlated signal and the SIN (or IMAGINARY) component. A rectangular to polar conversion makes these two data channels equivalent to the amplitude and phase of the correlated signal. Optional phase rotation of the 1 MHz reference frequencies permits compensation of the natural fringe rate caused by the earth's rotation and introduction of a fixed-period artificial fringe rate. This is convenient for real-time displays during fixed frequency operation. For frequency-agile observations, however, the natural fringe rate must be used. In either case, appropriate compensation is made during post-analysis.

Boxcar integration techniques are used so that successive measurements at 25, 50 or 100 ms intervals are completely independent. The digitized measurements are written to magnetic tape along with housekeeping information such as frequency, polarization, gain settings, phase-lock and antenna-tracking status, etc.

Typical observations consist of 90 minutes of continuous solar observations alternating with brief observations of a cosmic source to provide timely calibration of system phase and gain.

III. FREQUENCY-AGILE RECEIVERS

In the design of the overall system as outlined above, only the parabolic antennas and receivers are required to respond from 1 to 18 GHz. In this section, we describe the receiver concept which permits interferometry over this range.

A block diagram of the receivers is shown in Figure 3. Receiver functions are controlled by the computer which defines 23 bit control words sent to the receivers once every 48 microseconds over a serial data links.

Each receiver uses two feeds, one for right and one for left circular polarization. Each feed is a cavity-backed logarithmic spiral which responds over the range 0.5 to 18 GHz. The pair of feeds are mounted on a plate such that one feed is located at the focus. A variable-pitch gear and stepping motor can rotate this plate so as to rapidly and precisely interchange the feeds. A coaxial switch selects one of the two feeds as the source of the microwave signal. The signal corresponding to the desired polarization then passes through a rotary joint to the remainder of the receiver. At this point a noise diode with output over the range 1 to 18 GHz can be activated to inject a reproducible signal increment into the system for secondary calibration of system gain. The microwave signal is down converted to an intermediate frequency (IF) of less than 60 MHz using a wideband mixer-preamp and low-pass filter. The amplified output passes through a set of computer-controlled attenuators which cover the range 0 to 55 db in steps of 5 db. Combined with the intrinsic properties of the back-end hardware, this provides the dynamic range of 10^9 required to accomodate both cosmic sources and the full range of signal levels expected as a function of observing frequency and solar activity.

The observing frequency is determined by the local oscillator (LO) input to the mixer-preamp. Three YIG-tuned LO's are used to cover the range 1 to 18 GHz. Their output frequency is linearly related to tuning currents which are derived from a 12 bit integer specified by the computer. A pair of switches chooses which of the three LO signals is used.

This procedure determines the observing frequency to better than 5 MHz. For interferometry, however, the LO output must be phase-locked so that both receivers are observing coherently. To accomplish this, a 200 MHz reference signal is generated in the control room, amplified, split and sent to the two receivers (Figure 1). This reference signal provides the input to a harmonic

generator whose output includes all the harmonics of 200 MHz, extending over the range 1.0 to 18.0 GHz. Only one of these harmonics will be near the coarsely tuned LO frequency. Part of this LO output is mixed with the output of the harmonic generator. A phase-lock control circuit compares the mixer output (which contains the difference of the LO frequency and the nearby harmonic of 200 MHz) with the 1 MHz reference signal and then closes the feedback loop by fine-tuning the LO accordingly. In this way the observing frequency is phase-locked to $(N \text{ times } 200 \text{ MHz} - 1 \text{ MHz})$ where N is an integer (the harmonic number) in the range 5 to 90.

Frequency changes are initiated by the computer specifying a new coarse tuning current corresponding to a different harmonic of the 200 MHz reference. Frequency changes which do not involve switching between LO's take 16 ms with mechanical switching times adding another 30 ms when necessary. Polarization changes require 500 ms. The software synchronizes these changes with the data acquisition intervals of 25, 50 or 100 ms so that successive intervals can be devoted either to measurements or to frequency/polarization changes. Computer limitations currently restrict practical observations to the 50 or 100 ms integration time which permits up to 10 different frequencies per second to be observed.

It is worth emphasizing that frequencies are not swept in a continuous manner. Rather the system successively observes at discrete frequencies in a preprogrammed, but arbitrary order. This provides considerable flexibility in observing plans since such observing sequences can be optimized to trade-off time resolution, frequency-resolution and/or frequency coverage to match an experiment's objective or modified in real-time to reflect transient solar conditions.

IV. CALIBRATION AND DATA PROCESSING

In this section we discuss some of the procedures necessary to provide absolute calibration of the system outlined above. We also outline the data reduction process which converts the acquired data into calibrated spectra and light curves.

1. Frequency Calibration

Since the phase-lock system requires that the coarse tuning current be accurate to within about 9 MHz, it is necessary to accurately define the set of integers which

determine the coarse tuning current for each receiver at each harmonic. This process is aided by an audio-frequency feedback from the receiver phase-lock control to a computer interface. The audio frequency, proportional to the fine tuning current required to maintain phase-lock, is monitored by the computer which can optimize the coarse tuning current accordingly. Thus on a slow timescale, the computer can play an active role in the phase-lock process, so as to compensate for thermal drifts, etc. During frequency-agile operation, the computer also monitors the sequence of audio tones in order to flag any unsatisfactory phase-locks. In addition, the observer can literally listen to the phase-lock behavior, a feature which proved quite useful during early operations.

2. Total Power Calibration

The total power response as a function of frequency is determined by calibration on strong cosmic sources such as Cass A. The instrumental response is determined by Dicke switching between the on- and off-axis feeds when the on-axis feed is first on and then off the source. The difference of the differences then corresponds to the known flux of Cass A. (Suitable allowance is made for its partial resolution by 27 m dishes at the higher frequencies.) Since this process is quite time-consuming (approximately 5 minutes per frequency) noise diodes are used as secondary standards to monitor instrumental gain several times per day. Over a timescale of months, it was found that the relative gain as a function of frequency was stable to within a few percent over all but the extreme ends of the frequency range.

3. Polarization Calibration

Although the calibration procedure outlined above was accurate to better than ~10% in most cases, this level of precision is not satisfactory for polarization calibration. To obtain more precise polarization calibration, the relative response to the quiet sun was determined over a period of time. Assuming that the average quiet sun is unpolarized, this established the relative gain of the right and left polarized feeds (for extended sources).

4. Interferometric Calibration

Corresponding calibrations of stable interferometer parameters include the determination of the baseline, and of the relative phase and correlated gain as a function of frequency and polarization. These calibrations, based on cosmic sources such as 3C84, 3C273, etc., are also normalized to the noise diodes.

5. Interference

Since most of the observations occur outside the protected radio-frequency bands, consideration must be given to the effects of external interference. Observing programs to evaluate such effects as a function of frequency, time and antenna orientation are currently underway. The preliminary results indicate that total power observations of the sun are not seriously affected by interference. At the other sensitivity extreme, however, external sources typically affect about 10 of the 86 frequencies during interferometric observations of cosmic sources. As the sources of external interference become better characterized, we anticipate that suitable computer-controlled IF filtering can minimize even these effects.

6. Routine Calibrations

While the detailed frequency dependence of the instrumental parameters discussed above is not necessarily a simple function of frequency, preliminary indications are that the relative frequency dependence is quite stable. This permits calibrations during the actual solar observations to be limited to just a few frequencies, sufficient to determine the expected simple form of thermal and weather caused effects which vary on a timescale of hours. These more frequent calibrations, typically performed every 90 minutes, include phase and amplitude calibration on a cosmic source, noise diode calibrations to establish overall system gain and determination of the effective zeroes of the analog signal processing system. Under computer control, these routine calibrations require about 15 to 20 minutes.

7. Data Reduction

Data reduction on the Caltech Astronomy VAX computer consists of three basic steps, all of which can be done in one pass. The first step consists of editing to eliminate data samples that were flagged due to antenna tracking or phase-lock anomalies, saturated data samples or most commonly, samples during which a frequency change was in progress. Next, the data are calibrated on the basis of frequency-dependent gain tables, adjusted to reflect the appropriate routine calibration results. Finally the data at each frequency and polarization are averaged or interpolated to a common time so that the resulting spectrum is the best estimate of the instantaneous spectrum of a changing signal. (In general, we have found that the derived spectra are not sensitive to the interpolation technique.) At this stage, the data are in the form of a

calibrated matrix whose axes represent time and frequency/polarization respectively. Such data, which represent calibrated dynamic spectra, can then be further manipulated, or displayed as light curves, spectra, etc.

8. Spectral Smoothing

Evaluation of the spectra determined by this procedure must deal with the following complication. The current precision of ~10% for the intensity calibration of individual frequencies would be generally satisfactory for spectral analysis if the frequency resolution were low. However with frequency resolution significantly better than 10%, this level of precision causes the resulting spectra to appear unnecessarily 'noisy' at the 10% level. As an interim measure to permit easier evaluation of spectral features, we have found it useful to smooth the resulting spectra using an algorithm which makes no a priori assumptions as to its form or shape and which does not systematically affect either the average level or slopes of the spectra.

Finally, it should be emphasized that as of this writing the calibration of the interferometer is still at a very early stage. Considerable improvement in both precision and allowance for systematic effects is anticipated in the next few months.

V. DEVELOPMENT STATUS AND INITIAL RESULTS

In this section we briefly outline the development of the frequency-agile system, present some of the initial flare spectra obtained, and indicate modifications planned for the near future.

1. Early Observations

The first frequency-agile receiver became operational in April 1981. This receiver differed from those described above in that it contained a fourth LO, phase-locked at 10.6 GHz, in addition to the three YIG-tuned oscillators covering the range 1 to 18 GHz which were not phase-locked at that time. Until mid-1982, the system was operated in a 'hybrid mode' whereby this receiver provided high spectral resolution data in total power (no spatial resolution) while a fixed-frequency receiver on the other antenna provided high time resolution (50 ms) data at 10.6 GHz, and the combination provided interferometry at 10.6 GHz. Extensive solar observations in this mode between May and October 1981 provided high spectral resolution data for many flares.

2. Narrow-band Events

One of the early surprises found in this flare data were microwave events which we have tentatively called "narrow-band" microwave bursts. Previous observations of microwave spectra generally show events with spectral widths of ~100% of their peak frequency. We have found many microwave bursts with a relatively narrow FWHM bandwidth of ~60% or less. Such 'narrow-band' events feature sharp high- and low-frequency cutoffs. Alternatively, one can characterize the low frequency cutoff in terms of the quasi-cutoff frequency (the low-side frequency at which the flux is one tenth the flux at the peak frequency) defined by Guidice and Castelli (1975). For the narrow-band events the ratio of the peak-frequency to the quasi-cutoff frequency can be as little as 1.6, compared to an average of 3.4 (and a minimum of 2) previously found on the basis of low spectral resolution patrol data.

Figure 4 shows an example of the peak spectrum and corresponding light curves of a typical narrow-band event. The light curve from the HXRBS experiment on the SMM satellite shows a small corresponding hard X-ray burst which might suggest a non-thermal as opposed to thermal origin for the microwave event.

Narrow-band events are often seen as part of larger bursts. Considering the event in the top panel of Figure 5, for example, we see that at 2 and 8 GHz, the impulsive phase apparently did not begin until 190030 UT. When observations at the intermediate frequency of 4GHz are included, however, (bottom panel) we see that the event clearly began 4 minutes earlier. This apparent anomaly is resolved by the corresponding sequence of spectra shown in Figure 6, in which a narrow-band event, peaked at 4 GHz is seen to be responsible for the early emission. Considering the spectral development more closely, we find that the narrow-band component became observable at 185620 and rose until 185740. Forty seconds later, this component was unchanged, but an additional component, centred at 8 GHz had risen. The second panel shows that the 8 GHz component had disappeared by 185900, but by 190020 had developed once more, along with a separate component at 1.4 GHz and an increase in the original 4 GHz component. The separate components at 1.4, 4 and 8 GHz then evolved into the impulsive phase emission with its conventional wide bandwidth (third panel).

Such behavior has several interesting implications for our understanding of microwave bursts. First it illustrates that significant microwave emission can occur several minutes before the start of the main energy release.

Second, the narrow spectral widths would suggest that the narrow-band events originate in a region of relatively uniform physical conditions. Thus one might speculate that they are a form of elemental microwave burst. Third, the sharp low-frequency cutoff has implications for the physical origin of the spectral cutoff. For example, although gyrosynchrotron self-absorption can readily explain a low frequency spectral index of 2.5 to ~ 3 (Dulk and Marsh 1982), some of narrow-band events have low frequency spectral indices of over 5, thus requiring different explanations, such as Razin suppression, external gyroresonance or free-free absorption (Melrose 1980).

Fourth, the evolution of this event suggests that in some cases, wide-band spectra may be partially composed of a superposition of narrow-band events. In such circumstances, the interpretation of the wide-band spectra must be done with care. For example, it is possible that in some cases the evolution of spectral parameters might be due in part to the relative time-evolution of different narrow-band spectral components. Also, in cases where a wide-band source is partially composed of several components, one should not necessarily expect correspondence between images at widely spaced microwave frequencies.

3. Present status

Observations with the frequency-agile interferometer in the configuration described in sections II and III began in October 1982. The addition of two-element interferometry with high spectral resolution has added three capabilities to microwave spectroscopy. First, it suppresses signals from the extended, background sun to permit the interferometer to isolate the signals from compact sources of the nonflaring active region. Thus the system can conveniently determine the active region spectrum prior to or following flaring activity. Second it also provides a significant practical gain in sensitivity to extend the spectrum of small bursts to lower levels than is possible with a total power data. Third, since the separation of the antennas in units of wavelength is different at each frequency, measurements at each frequency sample different spatial Fourier components of the source. In cases where the spectrum is known, this provides an imaging capability. Although the practicality of such imaging remains to be explored, as a minimum it will permit the removal of lobe ambiguities normally associated with a two-element interferometer. For the narrow-band bursts, the application of this imaging capability will be of particular interest for establishing their spatial location and relationship to other aspects of the flare process. The interferometric results will be the subject of subsequent papers.

4. Future plans

Apart from incremental hardware/software improvements and expected refinements in calibration, the next major step in the exploitation of high spectral resolution microwave observations at OVRO is expected to occur by the end of 1983 with the completion of a third frequency-agile receiver, similar in design to the two already in service. The third receiver will be used on an occasional basis on the OVRO 40 m antenna in conjunction with the present system to permit three-element frequency-agile interferometry. The resulting set of three baselines at each frequency will add two further capabilities. First, it will extend the snapshot "imaging" capability to 2 dimensions, rather than one. Second, it will permit the determination of source size at each frequency and polarization. This in turn will enable the brightness temperature spectrum of solar bursts to be determined for the first time. Since this is the parameter that is derived from most theoretical models, we are hopeful that this will provide new scope for the effective interaction of theory and observation in the study of solar flares.

VI. ACKNOWLEDGEMENTS

Dr. Richard B. Read was responsible for the design and fabrication of the solar backend and frequency-agile receivers. R. M. Goeden developed the feed-switching mechanism. I am grateful to Dr. H. Zirin for his support and encouragement during the development of this system.

The work performed under this effort (Air Force Geophysics Laboratory Contract F19628-82-K-0033) makes use of OVRO observations funded by NSF Grants AST-7906345 and AST-8115969 and has benefitted from additional support from NSF Grant ATM-8108449.

VII. REFERENCES

- Dulk, G. A., and Marsh, K. A., 1982,
Astrophys. J., 259, 350.
- Guidice, D. A., and Castelli, J. P., 1975,
Solar Physics, 44, 155.
- Kaverin, N. S., Kobrin, M. M., Korshunov, A. I.,
and Shushunov, V. V., 1979, Solar Physics, 63, 379.
- Kruger, A., 1979, Introduction to Solar Radio Astronomy and
Radio Physics, D. Reidel, Dordrecht.
- Marsh, K. A., and Hurford, G. J., 1982,
Ann. Rev. Astron. Astrophys., 20, 497.
- Melrose, D. B., 1980, Plasma Astrophysics: Nonthermal
Processes in Diffuse Magnetized Plasmas, Volume 1,
Gordon and Breach, New York.
- Orwig, L. E., Frost, K. J., and Dennis, B. R., 1980,
Solar Physics, 65, 25.
- Schmahl, E., 1980, Radio Physics of the Sun,
(ed. M. R. Kundu and T. E. Gergely), Dordrecht, p71.
- Zirin, H. , Hurford, G. J., and Marsh, K. A., 1978,
Astrophys. J., 224, 1043.

FIGURE CAPTIONS

Figure 1. Simplified schematic of the two-element frequency-agile interferometer.

Figure 2. Interferometer configuration, showing the possible locations of the 27 m antennas (X) relative to the 40 m telescope (T).

Figure 3. Schematic outline of the frequency-agile receiver.

Figure 4. Left: Light curves at the frequencies shown at right for a subflare on 1981 July 21. The lower curve is the hard X-ray time profile as measured the HXRBS experiment on the SMM spacecraft (Orwig et al. 1980). Right: Microwave spectrum near the peak of the burst, with preflare levels subtracted.

Figure 5. Top: Light curves at 2 and 8 GHz for a Class M3.9, Importance 2B flare of 1981 August 7. Bottom: Same time profiles with the addition of the intermediate frequency of 4 GHz.

Figure 6. Sequence of microwave spectra corresponding to the event shown in Figure 5.

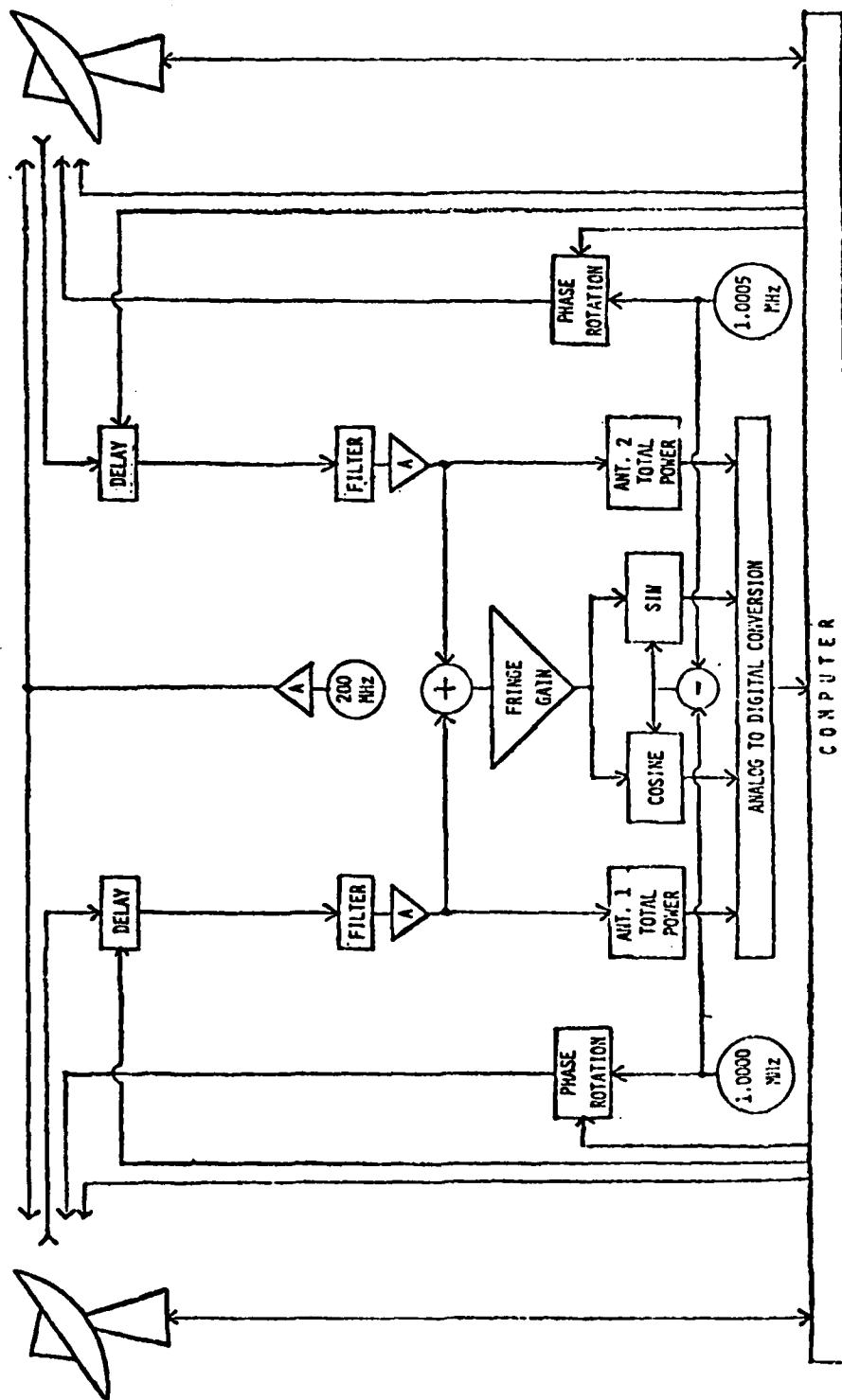


Figure 1

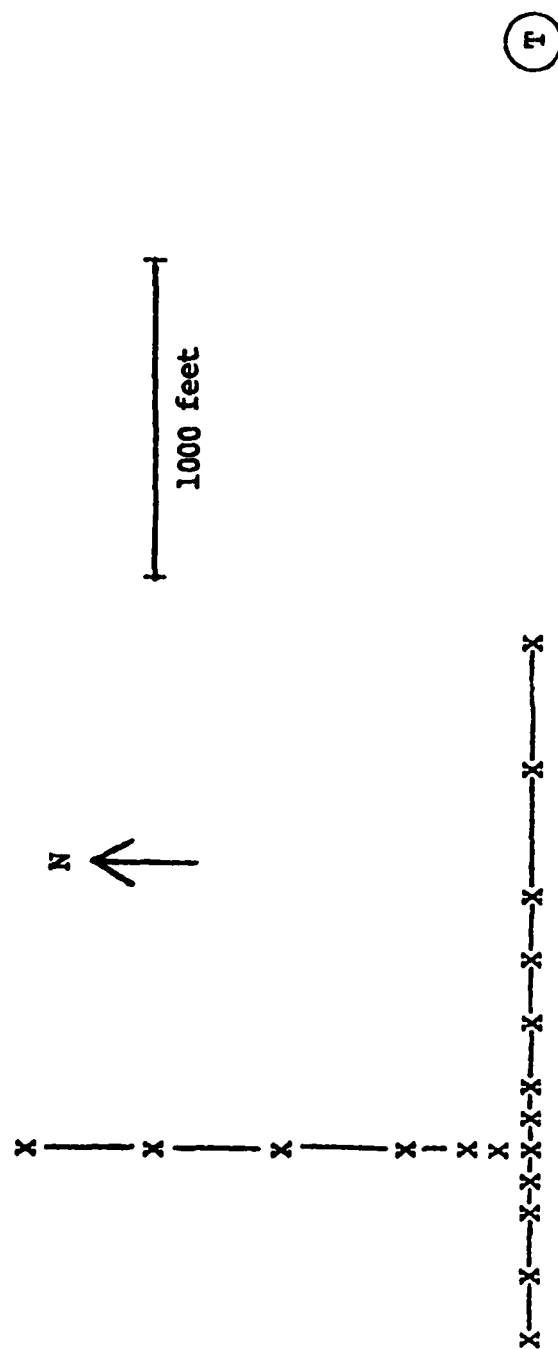


Figure 2

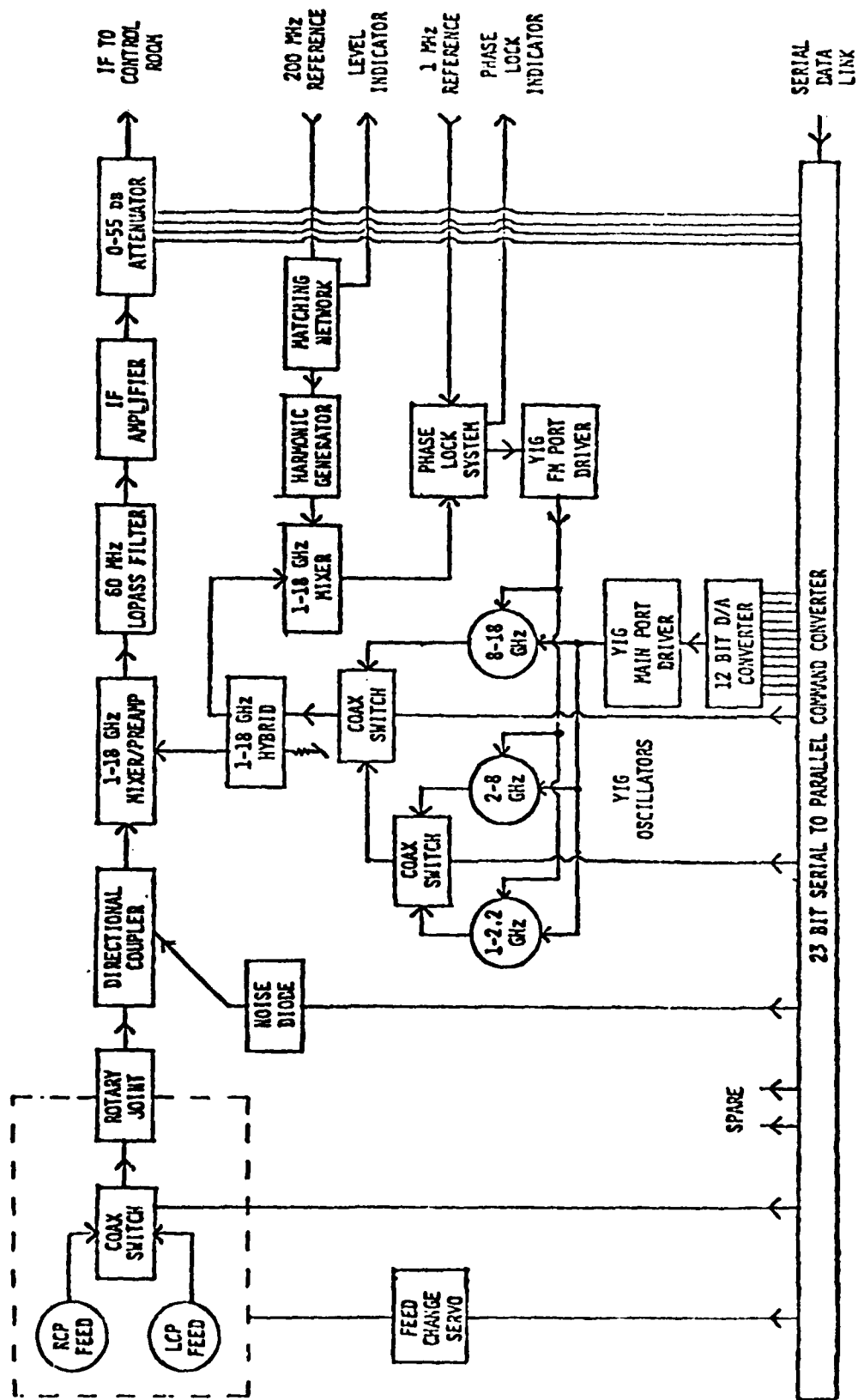
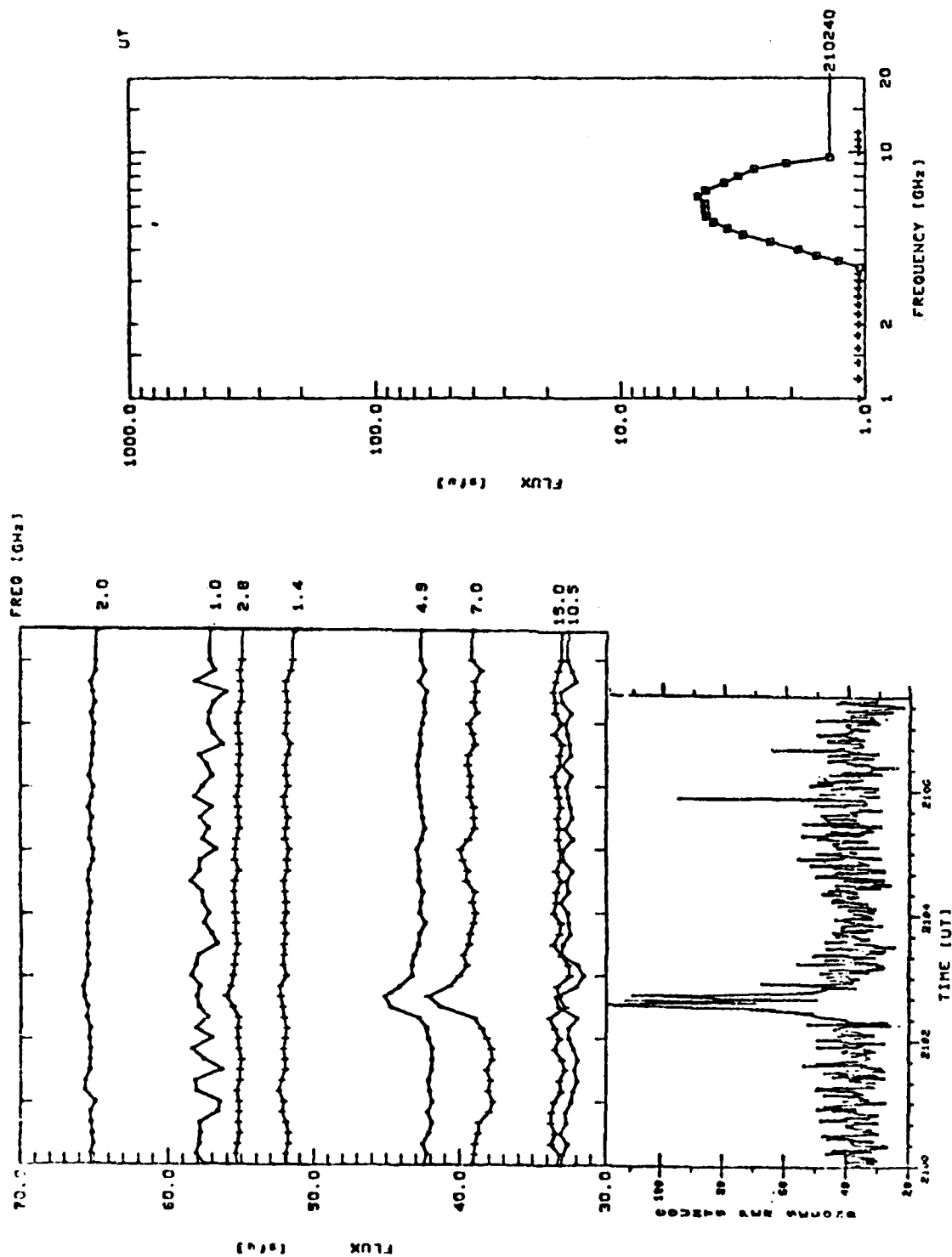


Figure 3



JULY 21 1981

Figure 4

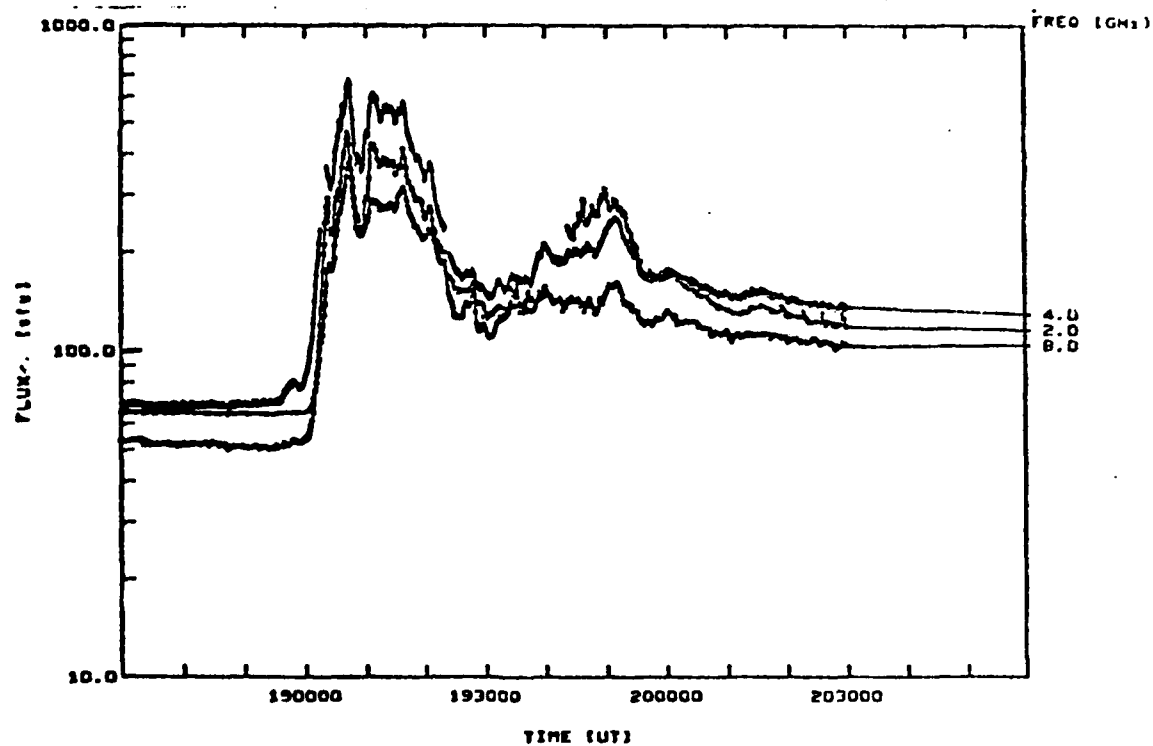
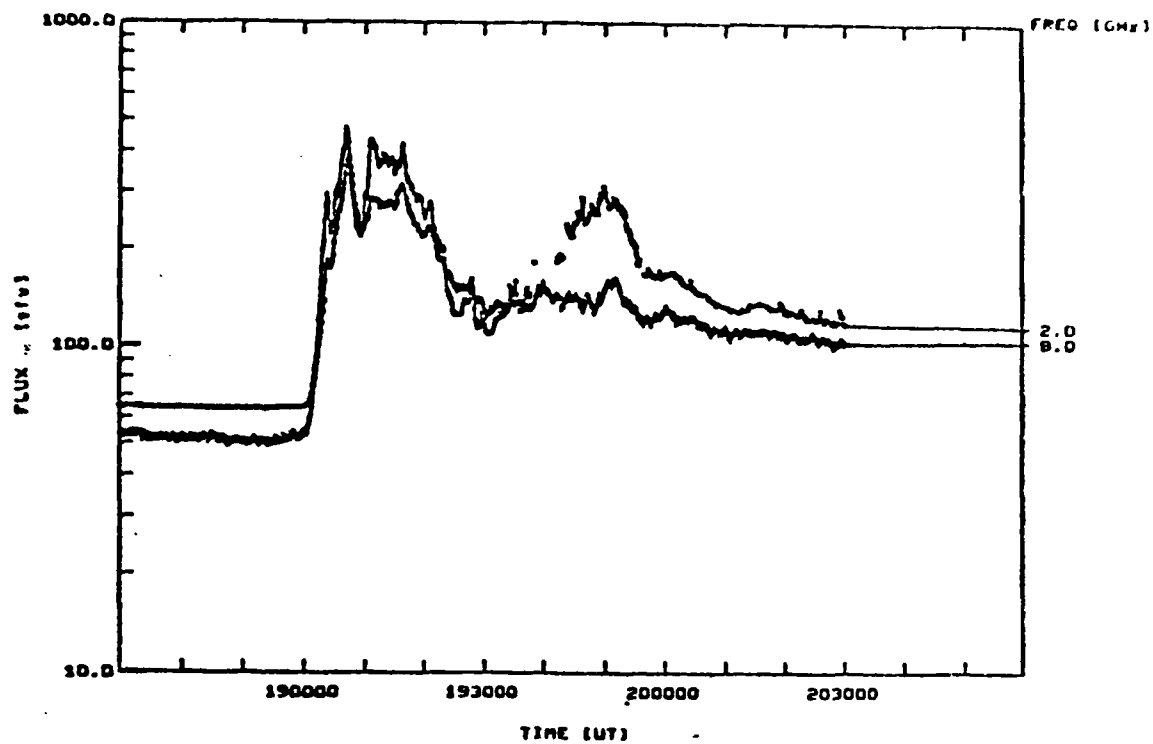


Figure 5

AUG 7 1981

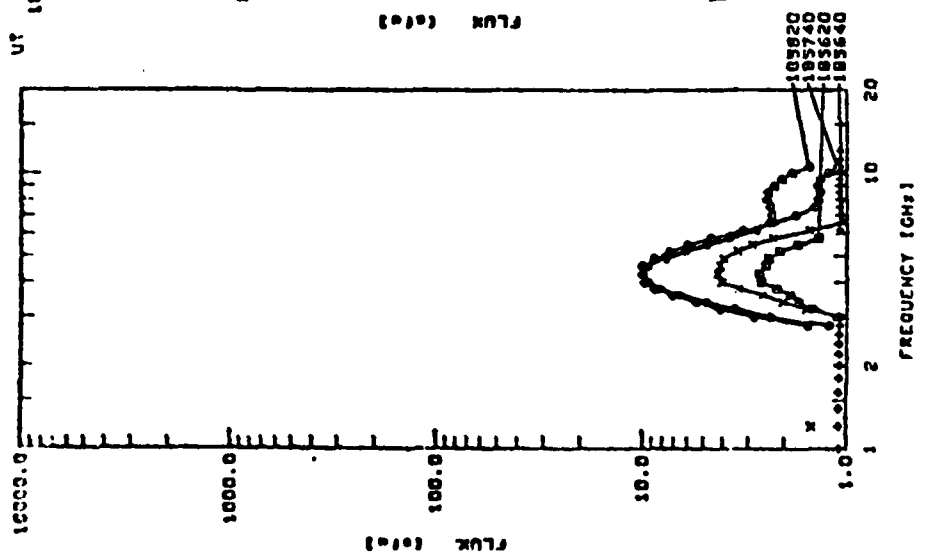
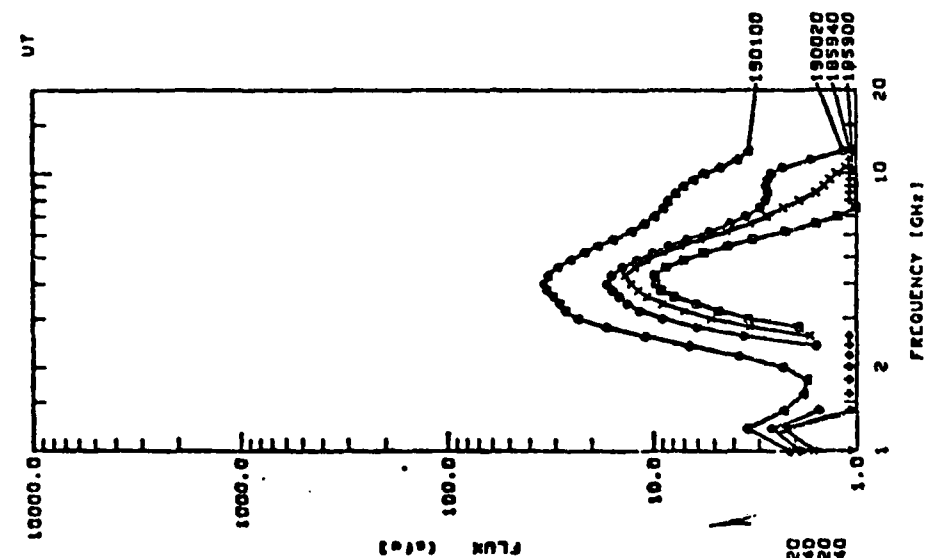
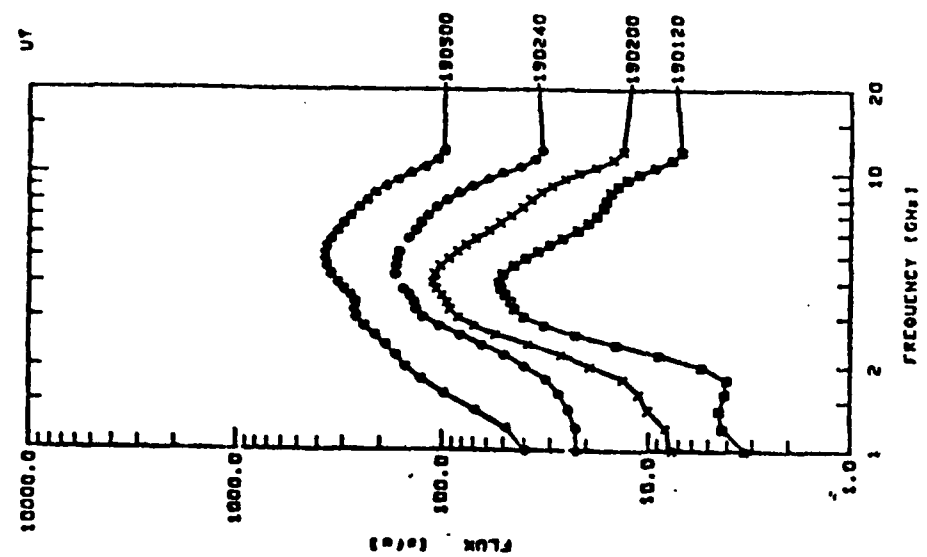


Figure 6

END

FILMED

9-83

DTIC